Modeling and Optimization of a Semiregenerative Catalytic Naphtha Reformer

Unmesh Taskar and James B. Riggs
Dept. of Chemical Engineering, Texas Tech University, Lubbock, TX 79409

Modeling and optimization of a semiregenerative catalytic naphtha reformer has been carried out considering most of its key constituent units. A detailed kinetic scheme involving 35 pseudocomponents connected by a network of 36 reactions in the C_5-C_{10} range was modeled using Hougen-Watson Langmuir-Hinshelwood-type reaction-rate expressions. Deactivation of the catalyst was modeled by including the corresponding equations for coking kinetics. The overall kinetic model was parameterized by benchmarking against industrial plant data using a feed-characterization procedure developed to infer the composition of the chemical species in the feed and reformate from their measured ASTM distillation data. For the initial optimization studies, a constant reactor inlet temperature configuration that would lead to optimum operation over the entire catalyst life cycle was identified. The analysis was extended to study the time-optimal control profiles of decision variables over the run length. In addition, the constant octane case was also studied. The improvement in the objective function achieved in each case was determined. Finally, the sensitivity of the optimal results to uncertainty in reactor-model parameters was evaluated.

Introduction

Catalytic naphtha reforming is practiced extensively in the petroleum-refining industry to convert gasoline boiling-range low-octane hydrocarbons to high-octane gasoline compounds for use as high-performance gasoline fuel. This is accomplished by conversion of *n*-paraffins and naphthenes in naphtha to isoparaffins and aromatics over bifunctional catalysts such as Pt/Al_2O_3 or $Pt-Re/Al_2O_3$. Recent environmental legislation in the United States has banned the use of lead as an additive for boosting antiknock properties of motor fuel. Coupled with these stricter environmental regulations, there has been a consistent increase in the demand for higher fuel efficiency standards of engines. This requires the use of higher compression ratios in engines, and therefore motor fuel with an even greater octane number. These considerations have continually forced the refiner toward producing higher-octane-number products from their catalytic naphtha reformers. This can be achieved by reforming the naphtha under more severe conditions, but this will also cause an increase in the rate of coke deposition, resulting in the reduction of cycle lengths of the catalyst. Due to these trade-offs and others, there is ample potential for optimization of a catalytic naphtha reformer. A proper selection of operating conditions within plant constraints is essential to maximize the profitability of the reformer. Due to the catalyst deactivation with time, the process assumes a transient nature and its optimization results in a time-optimal problem. This makes the optimization problem more challenging to solve. However, in the absence of an analysis of this kind, the unit may remain under suboptimal operating conditions, resulting in significant economic losses.

Use of mathematical models as a tool for either off-line or on-line optimization analysis is growing rapidly in the refining and petrochemical industries. A mathematical model requires various amounts of process knowledge and investment of time and effort, depending upon the level of complexity incorporated into these models. The advantage of utilizing rigorous mathematical models as compared to empirical approaches is related to the fact that the prediction accuracy of rigorous models can be significantly superior over a wide operating range. Hence, detailed mathematical models are frequently employed for optimization studies. In this work, a rigorous mathematical model of a semiregenerative catalytic reformer, based on fundamental physicochemical concepts,

Correspondence concerning this article should be addressed to J. B. Riggs.
Current address of U. Taskar: Aspentech, Inc., Houston, TX.

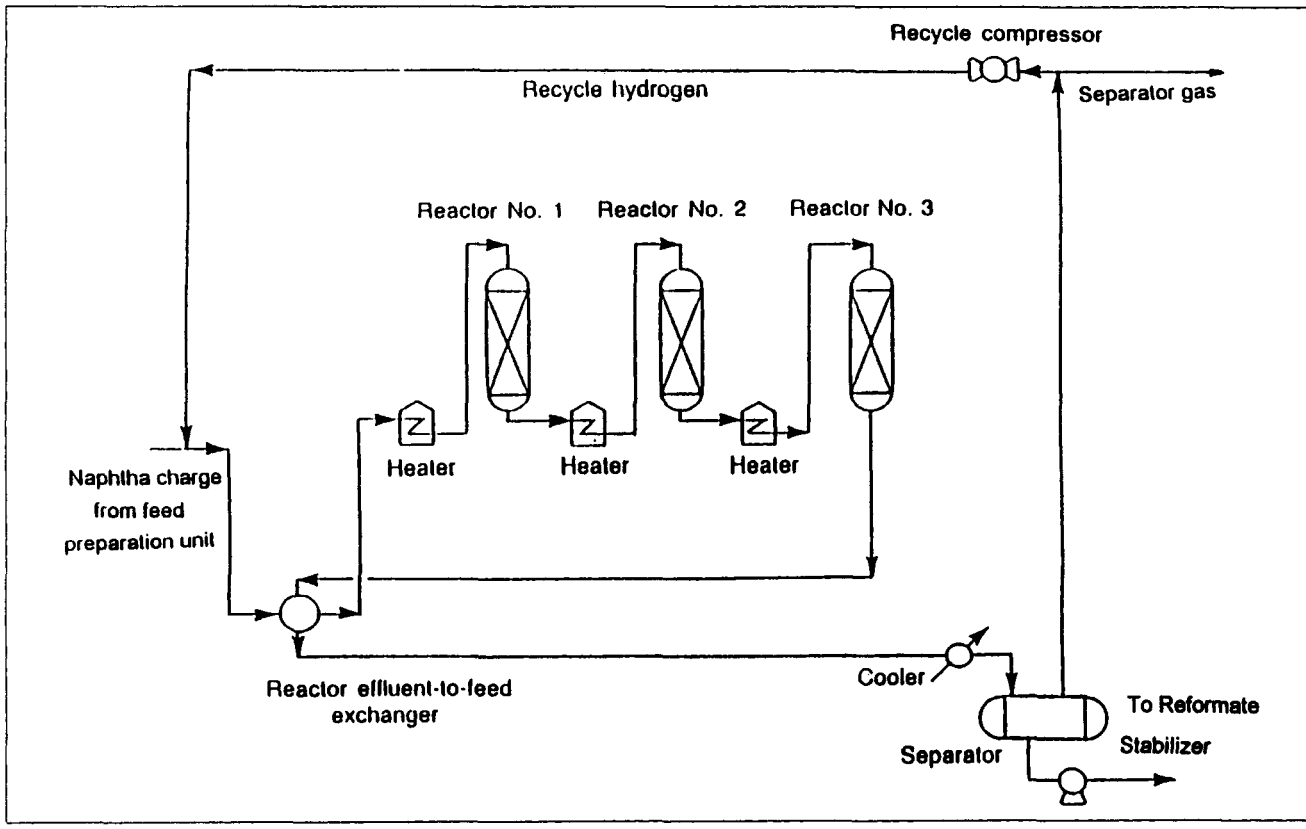

Figure 1. Process flow scheme of the catalytic naphtha reformer.

has been developed and utilized to conduct optimization studies. The model parameters were estimated on the basis of data obtained from an industrial unit. The modeling of the complex chemical reactions occurring on the surface of the bifunctional catalytic naphtha reforming catalyst during reforming was the most intricate part of the overall modeling effort. Appropriate kinetic modeling of these reactions was imperative in achieving the desired prediction accuracy of the model. A number of different approaches of varying levels of sophistication have been developed in the past to model the reforming chemistry (e.g., Smith, 1959; Krane et al., 1960; Kmak, 1972; Marin et al., 1983; Ramage et al., 1987). In addition, a variety of modeling schemes have been attempted to represent the deactivation phenomena on the surface of the reforming catalyst (DePauw and Froment, 1974; Beltramini et al., 1991). The kinetic scheme employed in this modeling work was largely based on previously published studies.

Catalytic Naphtha Reforming—Process and Chemistry

The process flow diagram of the reformer modeled in this work is shown in Figure 1. At the core of the reforming process are three or four fixed-bed adiabatically operated reactors in series that conduct the solid catalyzed vapor-phase reforming reactions. This is a semiregenerative type of unit, that is, the catalyst is regenerated periodically to compensate for the loss in activity of the catalyst due to coke deposition. The naphtha used as a catalytic reformer feedstock usually contains a mixture of paraffins, naphthenes, and aromatics in the carbon number range C_5 to C_{10}. The reformer-reactor charge is combined with a recycle gas stream containing 60 to 90 mol % hydrogen. The total reactor charge is heated, at first by exchange with effluent from the last reactor, and then in the first charge heater. The inlet temperatures of the beds vary between 750 to 790 K, and the reactors are operated at pressures of about 20 to 30 atm. The molar recycle ratio stated in terms of hydrogen to pure hydrocarbon feed varies from 4:1 to 8:1.

The major reactions in the first reactor, such as dehydrogenation of naphthenes, are endothermic and very fast, causing a very sharp temperature drop in the first reactor. For this reason, catalytic reformers are designed with multiple reactors and with heaters between the reactors to maintain reaction temperature at operable levels. As the total reactor charge passes through the sequence of heating and reacting, the reactions become less and less endothermic and the temperature differential across the reactors decreases. The effluent from the last reactor, at temperatures from 750 to 790 K, is cooled to 315 to 320 K, partly by heat exchange with the reactor charge. The stream then enters the product separator where flash separation of hydrogen and some of the light hydrocarbons (primarily methane and ethane) takes place. The flashed vapor, containing 60 to 90 mol % hydrogen, passes to a compressor and then circulates to join the naphtha charge. Excess hydrogen from the separator is sent to other hydrogen-consuming units in the refinery. The separator liquid, comprised mostly of the desired reformate product but also containing light gases, is pumped to the reformate stabilizer. Reformate off the bottom of the stabilizer is sent to storage for gasoline blending.

Most of the catalytic reactions in reforming involve rearrangement of the hydrocarbon skeleton, within the same carbon number group, except for the hydrocracking reactions, which crack the high carbon molecules into two lower-molecular-weight molecules. The dominant reaction types prevalent in catalytic reforming are dehydrogenation of naphthenes, isomerization of paraffins and naphthenes, dehydrocyclization (ring closure) of paraffins, and hydrocracking of paraffins. All the reactions produce an increase in octane number and all the reactions except isomerization of paraffins, result in a decrease in reformate yield. The fastest reactions are dehydrogenation, isomerization is moderately fast, while dehydrocyclization and hydrocracking are the slowest. The most rapid reactions (dehydrogenation) reach thermodynamic equilibrium, and the others are kinetically controlled. A high process temperature and a low pressure favor the thermodynamic feasibility as well as the reaction rate in the two most important reactions: dehydrogenation and dehydrocyclization.

Deactivation of catalysts by carbonaceous deposits is primarily caused by the blockage of active sites due to coke generated from the olefinic intermediates formed during the course of the main reforming reactions. Higher hydrogen pressures suppress the diolefin formation, reducing the coke formation. However, higher pressures reduce the selectivity to aromatics in the desired product. Overall, high temperatures and low pressures would seem most desirable for the main reforming reactions, but the same conditions favor deactivation of the catalyst. For this reason the process conditions should be a compromise between attaining a high-octane-number product and controlling the rates of catalyst deactivation.

Kinetic Modeling of Reactions

An effective kinetic reforming model must properly represent all the major types of reactions, recognize the fact that this is a solid catalyzed gas phase reaction system, and account at least for the most important classes of chemical species present in the reaction mixture. The large number of reactions and hundreds of components taking part in the actual reaction system make this a rather complex problem. In view of the kinetic model's ability to significantly affect the accuracy of predictions over a wider operating range, a careful consideration was applied in selecting an adequate kinetic scheme. To reduce the complexity of the model to a manageable level, the large number of chemical components are assigned to a smaller set of kinetic lumps, each composed of chemical species grouped together according to some criteria.

The first significant attempt at delumping naphtha into different constituents (Smith, 1959) considered naphtha to consist of three basic components: paraffins, naphthenes, and aromatics. Due to its simplicity, this model has been used in some recent reformer modeling work (Bommannan, 1989). However, the fact remains that it oversimplifies the nature of the process. In a more extensive attempt to model reforming reactions of whole naphtha, Krane et al. (1960) recognized the presence of various carbon numbers from C_6 to C_{10} as well as the difference between paraffins, naphthenes, and aromatics within each carbon number group. The model derived by Krane et al. (1960) contained a reaction network of twenty different components. All the models constructed up to this time were pseudohomogeneous in nature. Kmak (1972) presented the first endeavor to incorporate the catalytic nature of the reactions by deriving a reaction scheme with Hougen-Watson Langmuir-Hinshelwood type of kinetics. Rate equations derived from this type explicitly account for the interaction of chemical species with the catalyst. In another notable effort, Ramage et al. (1987) developed a detailed kinetic model based on extensive studies of an industrial pilot-plant reactor.

The Kmak (1972) model was later refined by Marin and coworkers (1983), who presented the reaction network for the whole naphtha, containing hydrocarbons in the carbon-number fraction from C_5 to C_{10}. The reaction network included 23 pseudocomponents and used Hougen-Watson-type rate equations. Marin and Froment (1982) and Van Trimpont et al. (1988) also conducted separate studies on C_6 and C_7 carbon-number fractions, respectively, and developed the corresponding Hougen-Watson-type rate equations. Various possible reaction paths and mechanisms were systematically evaluated before choosing the one that best fit the experimental data on a laboratory-scale reactor.

The lumping criteria discussed by Kuo and Wei (1969) was used for defining kinetic lumps for the complex-reaction system. Even though these expressions are quite complex in nature, it was perceived that the construction of reaction paths and rate expressions as illustrated by Marin and Froment (1982) and Van Trimpont et al. (1988) would incorporate the mechanistic insight to a maximum extent within the model. This would be expected to result in better overall prediction capabilities of the model. Therefore, this kinetic scheme was chosen to represent the reforming kinetics in the present study. In this work, the form of the rate expressions for C_6 and C_7 used were similar to those published (Marin and Froment, 1988), while the rate expressions for carbon-number fractions from C_8 to C_{10} used in this work are based on using rate expressions that have the same form as the C_6 and C_7 rate expressions.

Finally, the complete, detailed reaction model symbolizing the main reforming reactions of the components of naphtha with carbon numbers from C_5 to C_{10} consisted of a total of 35 pseudocomponents connected together by a network of 36 reactions. The pseudocomponents are listed in Table 1. The paraffins, naphthenes, and aromatics within each carbon number fraction were treated separately. The paraffins in each carbon-number group were divided into three individual pseudocomponents: straight chain, single branched, and multibranched. The five-carbon ring naphthenes were considered differently than the six-carbon ring naphthenes. As an example of the type of reaction network, and the form of rate expressions employed, Table 2 lists the reaction rate equations for the C_7 carbon number fraction. As an additional example, Figure 2 shows the reaction scheme for C_8. All the rate equations are nonlinear pseudomonomolecular in nature, with the rate coefficients obeying the Arrhenius law. The thermochemical properties of each lump were computed by taking a simple arithmetic average of the properties of the corresponding pure chemical components constituting the lump. Microscopic reversibility is satisfied with equilibrium constraints calculated from free-energy data by using the van't

Table 1. Chemical Species Considered in the Study

Chemical Component
C_5 fraction
n-Pentane
Isopentane
C_6 fraction
Multibranched hexanes
Single-branched hexanes
n-Hexane
Five-carbon ring C_6 naphthenes
Benzene
C_7 fraction
Multibranched heptanes
Single-branched heptanes
n-Heptane
Five-carbon ring C_7 naphthenes
Six-carbon ring C_7 naphthenes
Toluene
C_8 fraction
n-Octane
Single-branched octanes
Multibranched octanes
Five-carbon ring C_8 naphthenes
Six-carbon ring C_8 naphthenes
C_8 aromatics
C_9 fraction
n-nonane
Single-branched nonanes
Multibranched nonanes
Six carbon C_9 naphthenes
C_9 aromatics
C_{10} fraction
n-decane
Single-branched decanes
Multibranched decanes
Six-carbon ring C_{10} naphthenes
Naphthenes
Cracked light gases

Table 2. Reaction-rate Equations Obtained by Analyzing Experimental Conversions for C_7 Hydrocarbons

Type of Reaction	Reaction-Rate Expression
Isomerization of paraffins	$r = A_0 e^{-E/RT}(P_A - P_B/K_{A-B})/\Gamma$
Hydrocracking of single-branched and multiple-branched paraffins	$r = A_0 e^{-E-RT}(P_A P_H)/\Gamma$
Ring closure of *n*-paraffins	$r = A_0 e^{-E/RT}(P_A P_B P_H/K_{A-B})/\Gamma$
Ring expansion of alkylcyclopentanes to alkylcyclohexanes	$r = A_0 e^{-E/RT}(P_A - P_B/K_{A-B})/\Gamma$
Dehydrogenation of methylcyclohexane	$r = A_0 e^{-E/RT}(P_A - P_B P_H^3/K_{A-B})/(P_H\theta)^2$

Source: Van Trimpont et al., 1988.
Adsorption term for the acid function
$\Gamma = (P_H + K_{C_6-} P_{C_6-} + K_{P_7} P_{P_7} + K_{N_7} P_{N_7} + K_{TOL} P_{TOL})$
Adsorption term for the metal function
$\theta = 1 + K_{MCH_1} P_{MCH} + K_{MCH2}(P_{MCH}/P_{H^2})$
A_0 = Preexponential factor
E = Exponential factor
P_i = Partial pressure of component I
K_{i-j} = Equilibrium constant for $i \Leftrightarrow j$
A = Reactant
B = Product
H = Hydrogen

Hoff equation (Sandler, 1989). The heats of reactions are computed by utilizing the heats of formation of each species at standard temperature, and then computing them at the reaction temperature by using constant-pressure-specific heat coefficients of the gases. The distribution of individual gases like methane, ethane, propane, butanes, iso- and *n*-pentanes in the cracked products was decided on the basis of cracked-product distribution data published by Van Trimpont et al. (1988). The reformate octane was calculated as a molar average of the component octane numbers (Maples, 1983).

A considerable effort has been directed in the past on the study of the coking of platinum/alumina reforming catalyst (e.g., Beltramini et al., 1991). De Pauw and Froment (1974) developed a methodology of characterizing the deactivation of a catalyst by coke deposition in the isomerization reaction of *n*-pentane. Marin and Froment (1982) and Van Trimpont et al. (1988) applied this methodology to characterize the deactivation of the catalyst for reforming of C_6 and C_7 hydrocarbons, respectively. The distinctive feature of the approach used by the authors is that the deactivation functions are related to the real cause of deactivation, which is the actual amount of coke formed on the surface of the catalyst and not the process on-stream time as is usually done. This deactivation model was adopted in the present work for modeling the coking kinetics on the surface of the catalyst. A deactivation function ϕ_c, which varies between 0 and 1, is used to multiply the rates of the main reforming reactions calculated without deactivation. The deactivation function is related to the coke content by an exponential function of the type $\phi_c = e^{-\alpha Cc}$, where α is the deactivation constant and Cc is the coke content described as the weight of coke per unit catalyst weight. The coke content is evaluated by integrating the following differential equation in time:

$$\frac{dCc}{dt} = r_c, \tag{1}$$

where r_c describes the rates of coking reactions (Van Trimpont et al., 1988). An important fact to be considered here is that the deactivation function depends on time, since coke continues to deposit with time, as well as on the local temperature, pressure, and composition in the vicinity of the catalyst site. Thus, the deactivation function also varies axially

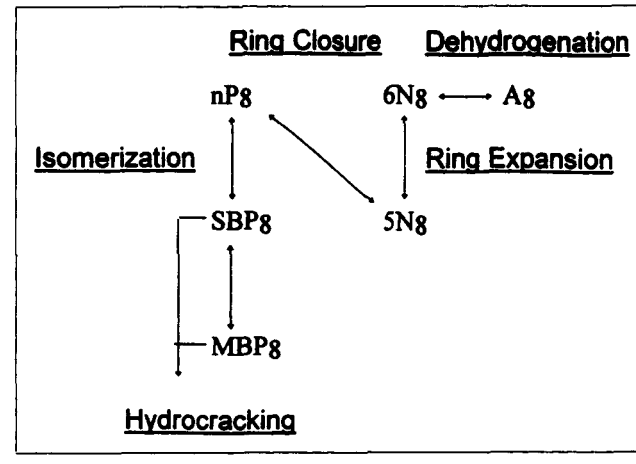

Figure 2. Reaction patch for C_8.

along the reactor length. For the purposes of simulation in this work, considering each bed to consist of two to three different regions of finite dimension, with each region represented by an average coke content, was found to be a reasonable way to accommodate the axial variation of coke content. The temperature profile in each bed is steeper at the entrance and flattens toward the end. This fact was taken into account by considering the coke regions at the entrance of the catalyst bed to be smaller in dimension than the coke regions placed at the end of the beds. More details of the kinetic modeling approach used in this work can be found in Taskar (1996).

The Process Model

The kinetic model and the process model discussed in the last section were incorporated into an overall fixed-bed adiabatic reactor model that forms the heart of the reformer model. The change in the activity of the catalyst with time causes the process to exhibit dynamic characteristics. Hence the rigorous mathematical description of the reforming reactor would lead to the following set of coupled nonlinear partial differential equations in space and time;

$$\frac{\partial f}{\partial w} = g_m(T, P, C_c, f)$$

$$\frac{\partial C_c}{\partial t} = g_c(T, P, C_c, f)$$

$$\frac{\partial T}{\partial w} = g_T(T, P, C_c, f). \tag{2}$$

This complex system would be difficult to solve directly. However, the equations are separable by taking advantage of the widely different time scales of conversion and deactivation. Therefore, a quasi-steady-state approach was adopted, that is, mole and energy balance equations were solved at steady state assuming constant catalyst activity for the calculation.

Under the usual reactor operating conditions, radial and axial dispersion effects were found to be negligible. The uncertainty associated with diffusion effects in the catalyst pellets was lumped into the kinetic-rate parameters. Thus a perfect plug-flow behavior could be assumed. The following ordinary differential equations, which describe the steady-state variation of the 35 chemical species and the temperature, were integrated through each reactor bed:

$$\frac{df_i}{dw} = \sum_{j=1}^{n_r} \gamma_{i,j} r_j \qquad i = 1, 2, \ldots, n_c \tag{3}$$

$$\frac{dT}{dw} = \frac{\sum_{j=1}^{n_r} r_j(-\Delta H_{R_j})}{\sum_{i=1}^{n_c} F_i C_{P_i}}. \tag{4}$$

The Ergun equation (Fogler, 1992) for computing differential pressure drop in the fixed bed was added with these equations:

$$\frac{dP}{dw} = -\frac{G}{\rho d_p \phi^3}\left[\frac{150(1-\phi)\mu}{d_p} + 1.75G\right]\frac{1}{A_c \rho_c}. \tag{5}$$

This set of ordinary differential equations, 35 component balances, and two state variables, was solved simultaneously with Eq. 1. Gear's (1971) numerical integration scheme for solving stiff ordinary differential equations was employed to integrate the equations through each fixed-bed reactor. This integration approach was found to be considerately more efficient than using a fourth-order Runge-Kutta integrator (Riggs, 1994) due to the stiffness resulting from high operating temperatures. This model of the fixed-bed reactors was integrated with models of other key units in the flow sheet.

The product separator, which separates the hydrogen and some lighter gases from heavier products, was modeled as an isothermal flash operation. This involved solving a set of material-balance and vapor/liquid equilibrium equations simultaneously. The formulation of these equations is fairly straightforward and is illustrated in standard texts (Holland, 1981). A modified Redlich-Kwong equation-of-state approach (Soave, 1972) was used to compute the vapor/liquid equilibrium constants.

The modeling of the recycle gas compressor and the reactor effluent-to-feed exchanger was required mainly for estimating the compression cost and the fuel cost in the first charge heater, respectively. The rigorous modeling of these components was not deemed to be necessary; macroscopic energy balances were used to model these units. The recycle gas compressor is used to compensate for the pressure drop in the loop. The power consumption of the compressor was estimated on the basis of calculated adiabatic head and flow rate of recycle gases:

$$\Delta H_{\text{adiabatic}} = RT_{\text{inlet}}\left(\frac{k}{k-1}\right) \times \left[\left(\frac{P_{\text{out}}}{P_{\text{in}}}\right)^{\frac{k-1}{k}} - 1\right]. \tag{6}$$

A macroscopic energy balance of the reactor effluent-to-feed exchanger was utilized to compute the temperature of the reactor feed before entering the first charge heater. The fuel cost of the first charge heater could then be easily calculated as the sensible heat required to heat the gaseous stream from the outlet of the exchanger to the inlet of the first reactor.

The strategy implemented for flow-sheet computation is also known as the sequential modular approach (Reklaitis, 1983). There are certain advantages to writing the model in this manner because it simplifies the analysis of the problem and directly determines the calculation sequence. Each block of equations involves only a few streams associated with that unit. However, the disadvantage is that an iterative solution may be required, as in this case where a recycle is present, which significantly increases the computation time. It was determined that using the alternative open-equation-based method (Reklaitis, 1983) was not feasible due to the restrictions of the computing system regarding the maximum manageable number of simultaneous equations.

The overall program flow chart depicting the calculation sequence is shown in Figure 3. Once the recycle is converged, the product properties, such as volumetric reformate yield, and octane number of the reformate, are calculated. The re-

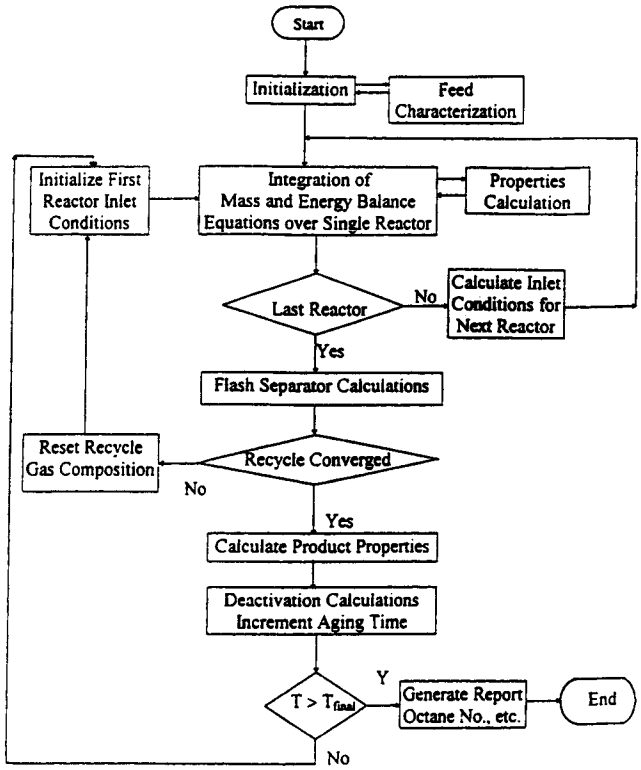

Figure 3. Program flow chart for the catalytic naphtha reformer.

formate octane number is computed as a volumetric average research octane number of the species present in the reformate.

Model Parameter Estimation

The objective of this study was to use the model, whose development has been outlined, to analyze the optimization issues relevant to an industrially operating catalytic naphtha reforming unit. It was therefore essential to benchmark the model against data obtained from an industrial unit. The choice of kinetic-rate parameters as adjustable parameters in the model was quite obvious since their values are seldom known exactly for a given system. Even the few cases where the values could be estimated directly from the published literature serve at best as good initial guesses for the parameterization procedure. The main adjustable parameters in the model were activation energies and preexponential factors of the main reforming reactions and coke formation reactions, and the adsorption equilibrium constants. Commercial data at start-of-cycle conditions were obtained from the Phillips Petroleum Company for one of their semiregenerative catalytic reformers.

A major limitation encountered with the data was the fact that all the data sets were clustered within a very narrow operating window rather than being spread over a wide operating region. This essentially amounted to having a single data set at the base-case operating point. An overall material balance, as well as hydrogen-balance closure, was checked to make sure that the chosen data set was internally consistent. The base-case operating conditions chosen for model-parameter estimation are listed in Table 3.

Table 3. Feed and Reformate Analysis and Flows from the Industrial Data

	Units	Feed	Reformate
ASTM distillation data			
0%	°F	230	112
10%	°F	246	178
30%	°F	257	237
50%	°F	271	267
70%	°F	289	290
90%	°F	320	323
100%	°F	356	406
API Gravity		52.4	42.4
PNA Analysis			
Paraffins (P)	mol %	49.67	34.36
Naphthenes (N)	mol %	29.72	1.93
Aromatics (A)	mol %	20.06	63.71
Flow	bbl/h	626	499

SI conversion: °C = (°F − 32)/1.8; L = bbl × 159.

Reactor-bed Temperatures, Pressure, and Catalyst-bed Weights

	Units	First Bed	Second Bed	Third Bed	Fourth Bed
Inlet temperature	°F	921	920	920	920
Outlet temperature	°F	812	880	909	916
Pressure drop	psi	3.3	3.1	3.0	5.0
Catalyst weight	lb	25,000	25,000	25,000	50,000

SI conversion: °C = (°F − 32)/1.8; kPa = psi × 6.89; kg = lb × 0.454.

The analysis of feed naphtha is usually reported in terms of its ASTM distillation curve and API gravity. Since the phenomenological model was written in terms of lumped chemical species, a feed characterization technique was implemented to infer the composition of the lumped species from the supplied naphtha analysis. The major steps followed in the characterization technique are listed below:

1. The ASTM distillation data were first converted to true boiling point (TBP) data.

2. The whole TBP curve was discretized into a number of volume fractions. Based on the reported API gravity of the whole mixture the specific gravity of each volume fraction was evaluated by means of the Watson-K-factor approach (Lion and Edmister, 1975).

3. Based on the average TBP of each fraction and its specific gravity, certain thermophysical properties, such as molecular weight, critical properties, and liquid molar volume, could be predicted by using the correlations of the form, $\theta = \alpha T_b^{\beta} \gamma^{\delta}$, where θ represents any of the properties just mentioned. The values of constants α, β, and δ required for computation of each property are given Riazi and Daubert (1980a).

4. Each TBP fraction would actually consist of a mixture of chemical species whose boiling points would fall within the TBP range of the corresponding fraction. A nonlinear optimization search was applied to seek the compositions of chemical species that would give the best match between the predicted and observed properties in each volume fraction. Once the composition of a chemical species in each of the volume fractions was known, its composition in the entire mixture could be easily calculated.

Table 4. Comparison between Calculated and Predicted PNA Analysis of the Feed

	Mole Fraction		Rel. Abs. Error
	Calc.	Given	
Paraffins (P)	48.2	49.67	3.04%
Naphthenes (N)	30.12	29.72	1.33%
Aromatics (A)	21.68	20.06	7.47%

Based on the calculated compositions of lumped chemical species in the feed, the total paraffin (P), naphthene (N), and aromatic (A) content of the stream was computed. A comparison to the P, N, and A analysis provided with the given data indicated a good match, with relative errors ranging from 1% to 7% (Table 4).

Since we only had a limited amount of data available for benchmarking, the number of unknown coefficients was more than the number of independent measurements available. Therefore, the number of unknown kinetic-rate parameters in the model had to be reduced. This was accomplished by following certain guidelines or heuristic rules that were developed from the large amount of information published in the past on the chemistry and relative rates of various reforming reactions (Hettinger et al., 1955; Parera and Figoli, 1994; Little, 1985; Turpin, 1994). These guidelines are:

1. Due to the very fast nature of the dehydrogenation reactions of naphthenes, they were considered to be at equilibrium at all times.
2. Within a given carbon number fraction, rate constants for all paraffin isomerization reactions were assumed to be equal. Similarly, rate constants for all the hydrocracking reactions within a carbon number fraction were considered to be equal.
3. The relative rates of dehydrocyclization reactions of paraffins increase almost linearly with the carbon number. The rate constants for carbon number fractions from C_6 to C_{10} were considered to be at a fixed ratio to the rate constants for C_8 fraction. In other words, once rate parameters for dehydrocyclization in C_8 fraction were determined, the rate parameters for dehydrocyclization reactions in all the other carbon-number fractions were set as fixed ratios of the rate constants for the C_8 fraction.
4. The activation energies of the paraffin isomerization reactions were considered to be equal irrespective of the carbon number. Similar arguments were also extended for naphthene isomerization and paraffin hydrocracking reactions.
5. The rate expressions accounted for adsorption of chemical species on the catalyst surface. A single adsorption equilibrium coefficient was used to describe the adsorption of all paraffins in the reaction mixture. Similarly, unique adsorption equilibrium constants were utilized to describe adsorption of naphthenes, aromatics, and cracked products on the catalyst surface, respectively.

After conducting the analysis just presented, the size of the parameterization problem was reduced to an extent where the number of unknown kinetic-rate parameters were reduced to 22 and could be fitted with the amount of data available. The available data were described in terms of the species flow rates at the outlet of the last reactor, which amounted to 28 data points. A standard nonlinear least-squares approach was adopted to regress the model coefficients by minimizing the weighted sum of squares between the observed and predicted values of molar flow rates of species at the outlet of the last reactor, and the temperature drops in each bed. The model parameters evaluated by the parameter-estimation algorithm are given in Table 5.

Table 5. Parameter Values Computed by Least-Squares Regression on Data in Table 1

	Activation Energy (A) kJ/mol	Pre-exp. Factor kmol/kg cat/h
Paraffin isomerization		
C_5		0.778×10^{8}
C_6		3.113×10^{8}
C_7	87.75	1.241×10^{9}
C_8		1.312×10^{9}
C_9		2.184×10^{9}
C_{10}		3.114×10^{9}
Ring closure for C_8	200.7	1.639×10^{16}
Naphthene isomerization		
C_7	256.4	6.994×10^{21}
C_8		7.012×10^{21}
Hydrocracking		
C_5		3.645×10^{15}
C_6		5.252×10^{15}
C_7	220.8	7.293×10^{15}
C_8		2.187×10^{16}
C_9		2.551×10^{16}
C_{10}		9.112×10^{16}
Adsorption equilibrium constant		
Paraffins	21.9	
Naphthenes	659.0	
Aromatics	70.3	
Cracked light gases	107	

The rate parameters for coke-formation reactions were acquired directly from the literature. The deactivation constant α was adjusted to match the predicted and observed decline in the activity of the catalyst based on the Phillips Petroleum plant data, which covered one month of operation.

Modeling Results

The temperature and composition profiles of paraffins, naphthenes, and aromatics along the reactor system are shown in Figures 4 and 5, respectively. These plots are based upon the base-case operating conditions in Table 3. The nearly instantaneous occurrence of dehydrogenation of naphthenes results in a sharp temperature drop at the entrance of the first bed and a corresponding sharp decrease in naphthenes concentration. The reaction mixture is reheated before entering the second bed, where most of the remaining naphthenes are dehydrogenated and a moderate temperature drop is observed. Paraffin dehydrocyclization reactions and accompanying hydrocracking reactions are the main reactions taking place in the third and fourth reactor, leading to the decrease in C_6+ paraffin concentration and an increase in cracked products present. The temperature and composition profiles predicted by the model agree quite well with those observed industrially (Mudt et al., 1995; Ramage et al., 1987).

The coke content on the surface of the catalyst in each bed for a sustained operation of 8,000 hours (approximately one

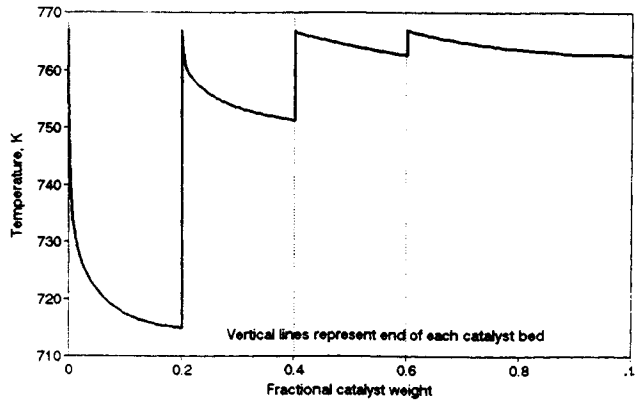

Figure 4. Temperature profile through reactor system.

year) was noted. The operating conditions prevalent at the base case (Table 3) were maintained over the entire period. As expected, the tendency for coke formation increases in going from the first to the last bed due to higher average temperatures in each successive bed and the accumulation of coke-forming components.

The sensitivity of the model output variables, such as octane number and reformate yield, to variations in process variables was studied over a wide operating range. A sensitivity analysis of this type provides an estimate of the gain of the process with respect to each of the process variables. Due to the lack of available operating data in different operating ranges, it was important to at least ensure that the process gains predicted by the model were in the proper direction. As an example, Figure 6 indicates the model-predicted variations for the research octane number and the volumetric reformate yield, with changes in the third-bed inlet temperature at the start-of-cycle conditions. As is usually observed, the octane number of the reformate rises with inlet bed temperature, but at a loss of the reformate yield. Figure 7 plots the octane number over the entire run length of the catalyst, but at different third-bed inlet temperatures with other conditions being maintained constant. At higher inlet bed temperatures, the octane number is higher in the beginning, but drops more rapidly later during the run. This is the result of significantly higher rates of coke formation expected at elevated temperatures. These results indicate the importance of

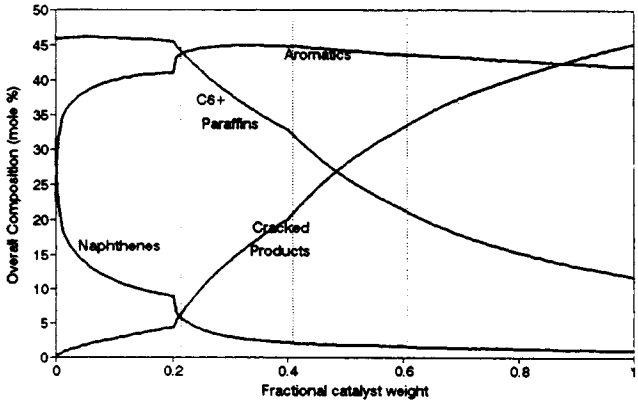

Figure 5. Profile of main component types through reactor system.

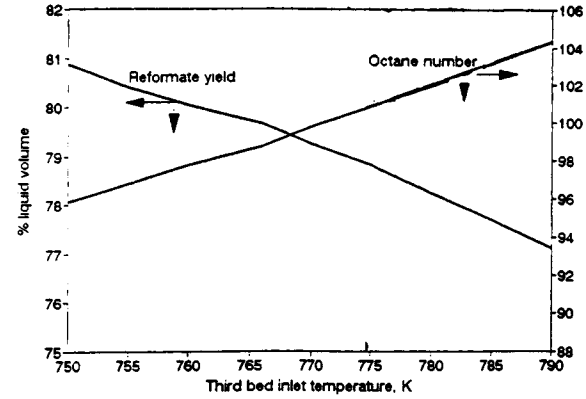

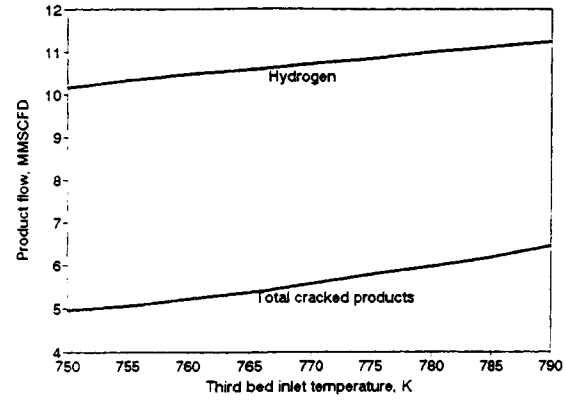

Figure 6. Sensitivity of products to third-bed inlet temperature.

maintaining the operating conditions that would achieve a proper balance between severity and catalyst activity.

Formulation of the Optimization Problem

The objective function was equated to the profitability of the unit by considering the prices of products and costs of utilities (Table 6). However, only the terms that could be influenced by varying the operating variables were included. The most significant product was the reformate, whose price was related to the quality, that is, the octane number. Other by-products in the process, such as hydrogen and cracked light gases, were also considered. The fuel cost and compression cost in the recycle gas compressor were accounted for in the objective function. The total objective-function value was evaluated by integrating the instantaneous value of the objective function from start of cycle till shutdown. The CPU time on a DEC-Alfa 150-MHz PC, required for computation of the total objective function over a one-year cycle length, was 15–20 min, depending on the operating conditions employed.

The objective in the optimization analysis was to find the operating policies within operational constraints such that the formulated objective function would be maximized. The decision variables for each optimization run were the four reactor inlet temperatures and the total recycle ratio. Some of the commonly encountered constraints in the actual operation of the catalytic naphtha reformer were enforced. The upper bounds of 790 K were considered on the reactor inlet tem-

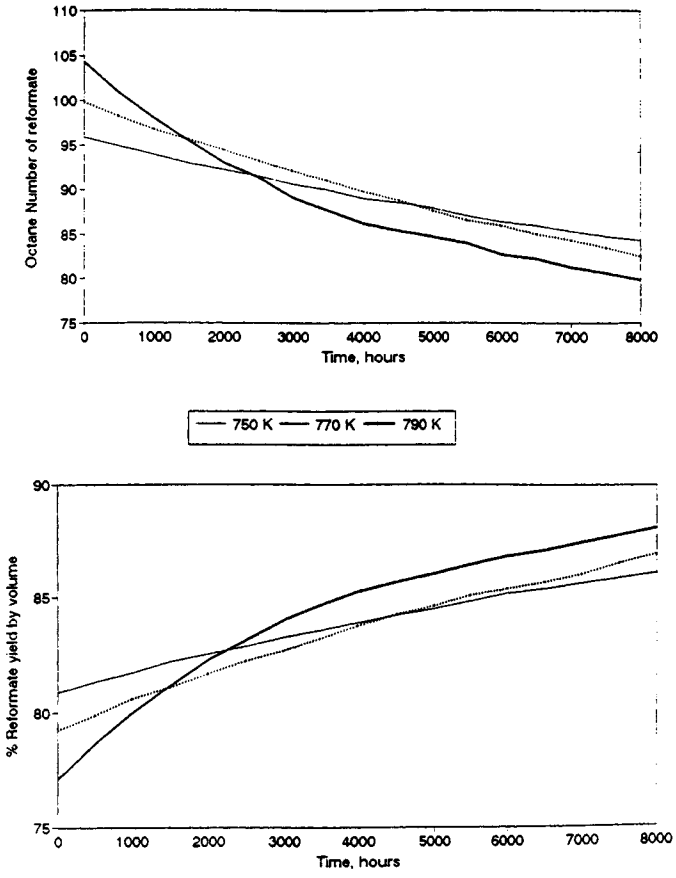

Figure 7. Sensitivity of products to third-bed inlet temperature over the catalyst life.

peratures, which correspond to the metallurgical constraints on the materials of construction. The upper bound of 8.0 was considered on the hydrogen-to-hydrocarbon feed recycle ratio. This is typical of the limits observed when recycle-gas-compressor capacity starts limiting the recycle flow. The time from startup to shutdown was considered to be predetermined. In other words, the catalyst life was imposed as an equality constraint for the problem. For a given optimization run, the feed conditions were assumed to remain constant over the entire run length. Also for a given optimization run, the separator pressure, which controls the pressure in the loop, was assumed to remain constant. The product prices and utility costs were also assumed to remain constant over the run length.

Table 6. Product Values and Operating Costs

Product Values	Operating Costs
Reformate	\$150/m^3 at 95
Octane value	\$4.5/OCT m^3
Hydrogen	\$71.8/KNM^3
Methane/ethane	\$7.8/gCAL
Propane	\$70/m^3
Butane	\$87.5/m^3
Fuel gas	\$7.8/Gcal
Compressor	\$0.08/kWh

SI conversion: J = cal × 4.19; MJ = kWh × 3.60.

Optimization Approach

Initially, the optimization analysis was conducted to optimize the plant only at start-of-cycle conditions. In other words, the issue that was handled was the possible trade-off between the octane number and the reformate yield. Obviously, deactivation of the catalyst did not feature in this problem. The results of optimization studies predicted all the inlet bed temperatures at the upper constraints, that is, the most severe operation was predicted as the optimum way to operate. However, it was quite clear that this mode of operation would seriously deactivate the catalyst in a very short time. In practice, the aim is to keep operating the unit until the planned shutdown, and maximize the overall profits. Thus consideration of the dynamic nature of the system caused by deactivation is essential to carrying out any meaningful optimization analysis of the problem.

Having concluded this, the optimization problem could still be viewed from several distinctly different perspectives. For the first one, which is referred to as the time-invariant mode of operation, the decision variables are maintained constant throughout the entire period of operation. The optimizer sought the five decision variables, four bed inlet temperatures, and total recycle ratio in this case, such that the objective function value over the entire run period was maximized. In actual practice, this would hardly be the preferred mode of operation. However, the analysis was useful from the point of view of addressing the following issue. Would it be advantageous to operate with a staggered reactor inlet temperature profile as compared to a uniform profile? In other words, the attempt was to locate the optimum inlet temperature configuration, rather than just the flat one, as is practiced sometimes in the industry.

The second optimization problem investigated, referred to as the time-optimal mode of operation, involved determining the optimal control profiles for the decision variables over the run length of the operation. The loss in activity of the catalyst with time causes the process to behave in an unsteady-state manner, requiring the solution of a dynamic programming problem. The most widely used numerical techniques to solve dynamic optimization problems are the collocation method (Biegler, 1990) and the control vector parameterization (CVP) method (Farhat et al., 1990). A review of the relative advantages and disadvantages of each method has been published in a number of references (e.g., Macchietto and Mujtaba, 1992).

Collocation methods discretize both the control functions and the ordinary differential equations in the original simulation model using collocation over finite elements. This approach approximates the state variables by a series of orthogonal polynomials in time. This converts a differential algebraic system to a large system of nonlinear algebraic equations, which together with the objective function and constraints, can be solved simultaneously using nonlinear programming (NLP) optimization techniques. A major advantage of this approach is the ease of incorporating constraints corresponding to the state and control variable profiles. The major difficulties of this approach are the size of the resulting NLP formulation and convergence reliability.

The control-vector parameterization method assumes a functional form for the input variables (polynomials, exponential, etc.), thus defining the time behavior of the input

variables over the entire run length. For example, a simple polynomial form may be used to represent the time-optimal path of an input variable u, such as,

$$u(t) = b_0 + b_1 t + b_2 t^2 + \cdots + b_p t^p. \quad (7)$$

The entire control profile is then defined by parameters from b_0 to b_p, and these form the decision variables of the optimization problem. The optimal control problem is then solved using the following sequential approach (Biegler and Cuthrell, 1985). A simulator of the process works sequentially with the NLP optimizer in order to provide information to compute the objective and constraint values and their gradients. The optimizer provides the values of the decision variables to the simulator, which defines the time history of the each input variable. The simulator then performs the simulation, calculates the objective function or constraint values as required, and returns them to the optimizer. The same procedure is illustrated by means of a simple block diagram in Figure 8. The advantage of this strategy lies in the reduced dimensionality of the optimization problem. However, it is difficult to enforce state- and control-variable constraints directly.

For the purpose of solving the time-optimal problem in this work, the control vector parameterization technique was utilized with a slight modification from the procedure described earlier. The continuous profile for each control variable is expressed in terms of node values at specific points in the time domain connected together by a smoothly varying interpolating polynomial. The optimizer uses these node values as decision variables, and as a result specifies each degree of freedom over the full range of time. The intermediate values for any particular control variable required by the simulator are provided by applying cubic spline interpolation (Riggs, 1994) between the node values for each control variable. Thus the entire path of each control variable is represented by a third-order polynomial with a spline. One advantage gained by this approach is that successive values of decision variables are connected by a smoothly varying function, and do not vary discontinuously over the operating region in a random fashion. It is also simpler to implement constraints on the decision variables because constraints on the original input variables just transform to constraints on the optimization decision variables (node values).

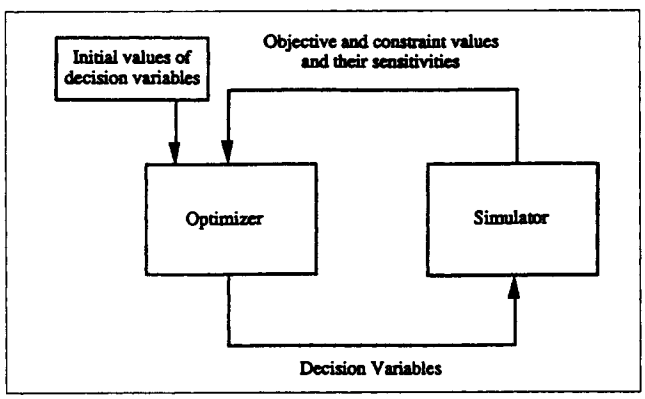

Figure 8. Optimization procedure.

The last mode considered is identical to the second mode, except that the product octane is constrained to a fixed value. That is, this mode involves the time-optimal allocation of the degrees of freedom for a fixed run time with the added constraint of a specified reformate octane level.

Optimization Algorithm

As mentioned earlier, one objective function evaluation took 15 to 20 minutes of CPU time. Therefore, it was necessary to choose an optimizer that, in general, required fewer functional evaluations for convergence. Sequential quadratic programming (SQP) was used to solve this nonlinear programming problem. It typically requires a smaller number of iterations than other comparable techniques, such as successive linear programming (SLP). SQP is usually much faster overall, particularly in cases where the optimum is not at a vertex of the constraints (Edgar and Himmelblau, 1988). Gill et al. (1986) have given a brief review of the theory behind the sequential quadratic-programming technique available as NPSOL 4.0, which was used in this work. At every major iteration of NPSOL, a quadratic programming subproblem is solved to find the search direction using a quasi-Newton approximation of the full Hessian. NPSOL is believed to be an extremely reliable code capable of handling up to several hundred constraints and variables (Nash, 1995). NPSOL 4.0 was found to provide efficient and reliable performance for the optimization problem of the catalytic naphtha reformer at hand.

Optimization Results for Time-Invariant Mode

The optimum value of the objective function found in every case is presented as a percent improvement over the one obtained at the base-case operating conditions, that is, assuming that the start-of-cycle conditions listed in Table 3 remain constant over the whole period of operation. The optimum operating conditions for the time-invariant mode of operation are given in Table 7. NPSOL typically required 50–60 function evaluation in order to solve the five-degree-of-freedom time-invariant case. The optimum objective function showed an improvement of 4.8% over the base-case operation (where inlet temperatures to all the beds are equal). This

Table 7. Optimum Operating Conditions for the Time Invariant Mode of Operation for Varying Feed Types

	Feed Type		
	Base	Heavy*	Light**
First-bed inlet temp.	790	790	790
Second-bed inlet temp.	779.7	777.6	780.1
Third-bed inlet temp.	766.8	765.9	767.3
Fourth-bed inlet temp.	766.9	763	767.1
Recycle ratio	9.96	10.85	9.53
% improvement in profitability over nominal† operation	4.8%	4.5%	5.4%

*Heavy means 10% increase in aromatics and 10% decrease in paraffins in feed.
**Light means 10% decrease in aromatics and 10% increase in paraffins in feed.
†Nominal operation involves using same inlet bed temperatures (767 K) for all the beds and a recycle ratio of 8.73 over the entire period of operation.

clearly indicated the advantage of maintaining a staggered reactor inlet temperature configuration over the uniform profile. The maximum inlet temperature was predicted for the first bed with successively lower inlet temperatures for each bed in series. This operation corresponds to the scenario where the coke buildup on all the beds proceeds at almost the same rate. The implication is that the optimum operation corresponds to the case where the catalyst activity in each bed is consumed almost equally.

Results were obtained at three different types of feed qualities: the base-case feed, the feed with a 10% increase in aromatics and a corresponding 10% decrease in paraffins, and the feed with 10% decrease in aromatics and a corresponding 10% increase in paraffins. It should be noted that despite small variations predicted in the operating conditions, the overall trend expected in each case remains the same, that is, maximum severity for the first bed and lower severity for each successive bed. The more aromatic feed seemed to favor slightly lower inlet temperatures than the lower aromatic feeds. This could be the result of higher coke-formation tendencies due to the more aromatic presence in the reactor. Also note that the lighter feed resulted in a more profitable optimum operation due to the resulting higher rate of reformate production.

Optimization Results for the Time-Optimal Mode

The control vector parameterization method based on cubic spline interpolation was used to solve the time-optimal problem. The first issue to be addressed was the determination of the number of node points for the time domain in the cubic spline interpolation for each degree of freedom. Initially, the analysis was performed with just three nodes, one each at the beginning and end of the cycle and one at the middle of the run. With three nodes for each of the five control variables, that is, the reactor inlet temperatures and the total recycle ratio, there were fifteen decision variables. The analysis was later extended to consider the case with four nodes for each control variable, that is, twenty decision variables to search for. A slight improvement in performance was observed due to the increased maneuverability achieved because of a larger number of nodes. Any attempt to extend the size of the problem beyond four nodes was found to increase the computational burden enormously without gaining any significant additional benefit. The predicted optimum-control profiles with four nodes are presented in Figure 9. NPSOL typically required 130 to 150 function evaluations in order to solve the 20-degree-of-freedom case using four node points for each input variable. Node placement is unequal with the nodes placed closer together toward the end of the run, due to more nonlinearity of the profiles in that region. The continuous line connecting the nodes indicates the optimum path predicted for each variable. The common trend observed for each bed inlet temperature is that the conditions at the start of the cycle are of lower severity, gradually moving toward higher severity, and almost reaching the upper inlet bed temperature constraint by the end of the cycle. Also, in terms of the severity of the inlet bed temperatures, the trend demonstrated was similar to the one displayed for the time-invariant case, that is, in general, going from the first to the last bed, inlet bed temperatures decreased.

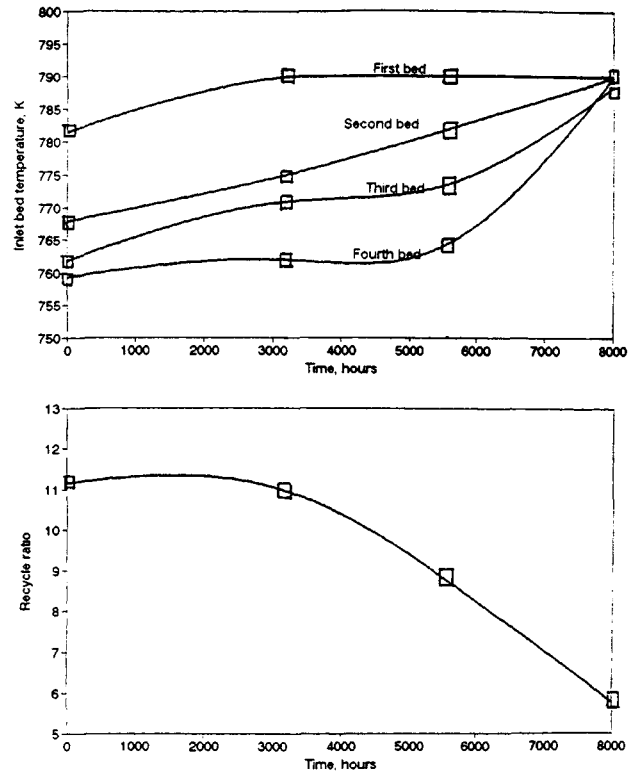

Figure 9. Time-optimal model of operation with increased node points.

The plot of octane number and volumetric reformate yield with time (Figure 10) provides additional insight into the operating mode selected by the optimizer. The operating conditions are varied in a manner such that the octane number remained more or less constant for a large part of the cycle. The continuous loss of catalyst activity during this period was compensated for by gradually raising the bed inlet temperatures. Toward the end of the catalyst life, the temperatures start increasing rapidly and the total recycle ratio drops, indicating the most severe operation. This can be explained by the following argument: since the time to shut down has been predetermined, it seems quite logical to use up all the available activity so as not to leave any unused activity before the

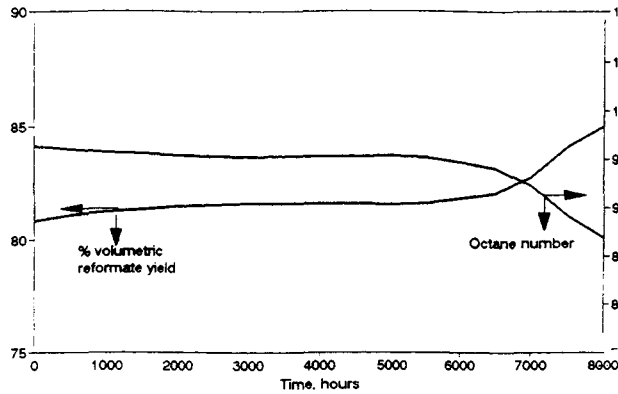

Figure 10. Product profiles for time-optimal mode of operation.

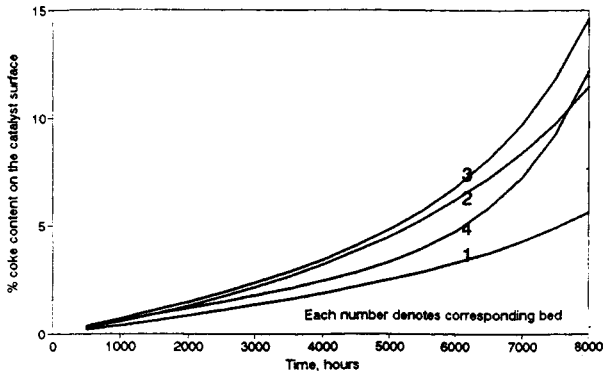

Figure 11. Coke content profiles for time-optimal model of operation.

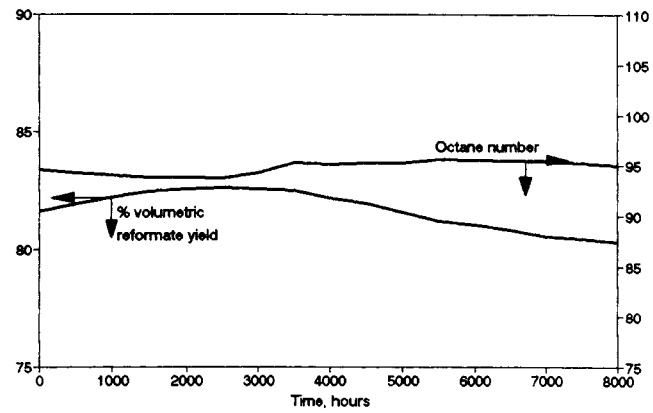

Figure 12. Product profile for fixed-octane mode.

regeneration. At the same time, the coke content in each of the beds needs to progress almost equally so that by the end of the run all the beds are almost completely deactivated. The coke content profiles under optimal conditions (Figure 11) support this conclusion. The increase in coke content is gradual at first and accelerates toward the end of the run. By the end of the run, the last three beds produce a heavy amount of coking with 12–15% coke content by weight, indicating that the catalyst activity is almost completely exhausted. The coke content of the last three beds increases almost at the same rate. The first bed shows the lowest coke content because its inlet temperature reaches the upper inlet temperature constraint much earlier in the run and cannot be raised further. As would be expected, the time-optimal mode is more profitable than the time-invariant operation. The time-optimal mode showed an additional improvement of 5.6% in objective function over the time-invariant mode.

Fixed-Octane Mode

The base case for the fixed-octane mode involved setting the inlet bed temperatures at the same value, but allowing that value to vary with time along with the recycle ratio in order to maintain the reformate near 95 octane for the length of the run. The time-optimal case was solved by using the control vector parameterization procedure for the reactor temperature and the recycle ratio such that the variation between the product octane and the target (95 octane) was minimized. It was found that the time-optimal case was able to maintain the specified octane only until the time equaled 6,500 hours instead of the full 8,000-hour run length.

The optimal results for the fixed-octane mode were obtained by setting each of the four inlet bed temperatures independently. The optimizer searched for the maximum profit conditions, while the 95 octane constraint was considered by adding a penalty function in terms of the reformate octane deviation to the economic objective function.

Figure 12 shows the optimal results for the fixed-octane mode. Note that there is some variation in the octane number of the reformate, but it generally stays close to a 95 octane. Note that after 3,000 hours of operation, the reformate yield decreased slowly from 82.5% to 80% in order to maintain the specified octane number. The optimal results showed only a 2.5% improvement in the economic objective function over the base case while staying closer to the octane constraint. The economic objective function for this case was based on the average profit per time over the full run length and a three week regeneration period. The advantage of the optimal approach largely comes from the fact that it was able to maintain the product octane for the full duration of the run since more of the inlet bed's activity was used. In general, there is little opportunity for economic optimization, since most of the economic maneuverability is consumed by meeting the constant reformate octane constraint.

Although these results were developed for a specified run time of 8,000 hours, in general, there will be an upper limit of run time for each specified octane level, where the higher the octane, the shorter the possible run time. An analysis of the optimum run-time length was not performed in this study.

Sensitivity Analysis

The optimization cases studied here clearly illustrate the potential for improving the profitability of the unit by conducting an analysis of this sort. However, the results are subject to the accuracy of the model coefficients, particularly the rate parameters of the reforming and coking reactions. A model-parameter sensitivity study was conducted to assess the impact of errors in some of the main parameters on the objective-function value. A 10% relative error was introduced in each parameter separately. The decision variable values found after the optimization analysis on this model using the time-invariant mode were substituted back into the original model (i.e., the model without any errors) and the objective-function value was reevaluated. As expected, this objective function value shows some deterioration from the original objective function value, which was found by performing the optimization analysis on the error-free model. The results of the sensitivity analysis are presented in Table 8. The uncertainties associated with the activation energies of the main reforming reactions showed a lower level of impact on the value of the objective function. The uncertainties associated with deactivation parameters had the largest effect on the results. However, in all cases the magnitude of the deterioration in the objective function indicated that the process profitability was not unduly sensitive to uncertainty in the model parameters.

Table 8. Model Parametric Sensitivity Analysis

Parameter	Rel. Error Introduced	Loss in Obj. Function Value*
Activation energy of ring closure reactions	10%	0.12%
Activation energy of hydrocracking reactions	10%	0.31%
Activation energy of paraffin isomerizatioin reactions	10%	0.05%
Activation energy of coke formation (Aromatics + Alkylcyclopentanes)	10%	0.85%
Activation energy of coke formation (Aromatics + Alkylcyclohexanes)	10%	0.79%
Deactivation parameter, α	10%	0.48%

*Note that the optimal time-invariant approach resulted in a 4.8% improvement in economic performance. The results listed here are the losses in economic improvement. For example, a 0.8% loss in objective function value would have resulted in a 4.0% economic improvement over the base-case operation.

Conclusion

A rigorous mathematical model of a semiregenerative catalytic naphtha reformer employing a detailed kinetic scheme was developed. The model was benchmarked with the industrial data to ensure that it adequately represented the actual plant variables at a base case operating point. The model behavior over a wide operating range was verified by comparison with the expected behavior in actual practice.

The time-invariant studies demonstrated that, due to the coking characteristics of reforming catalysts, a staggered use of inlet reactor bed temperatures clearly results in superior economic performance. More specifically, the bed temperatures should be set so that the inlet bed has the maximum allowable temperature with each successive bed at a lower inlet temperature. This approach results in a more uniform coking rate for each catalyst bed.

The time-optimal studies showed the same type of variation in inlet bed temperature as the time-invariant case, but the time-optimal studies varied the severity over the course of the run length. For the time-optimal mode, the severity increases gradually during the early stages of the run and eventually approaches the maximum severity at the end of the run. The time-optimal mode demonstrated significant economic improvement over the time-invariant mode. A sensitivity analysis indicated that the optimization results were most sensitive to uncertainties in the kinetic parameters associated with catalyst deactivation.

Finally, the overall conclusion of the work was that an optimization analysis of a regenerative catalytic naphtha reformer would be expected to result in significant economic benefits when the process is not operated in a constant octane mode.

Acknowledgments

This work was supported by the member companies of the Texas Tech Process Control and Optimization Consortium and the Center for Energy Research at Texas Tech University. The authors would like to thank Phillips Petroleum Company for providing the industrial data used in this study and Dr. Ed Sughrue, Phillips Petroleum Research and Development, for providing guidance during the model development phase of this work.

Notation

A_c = cross-sectional area of the catalyst bed, m^2
C_{Pi} = molar-specific heat of gases at constant pressure, kcal/kmol/K
d_p = diameter of catalyst particle, m
F_i = molar flow rate of species i, kmol/s
$\mathbf{f}$ = vector of molar composition of chemical species
G = superficial mass velocity of gases, $kg/m^2/s$
g = general function
k = ratio of specific heats of gases
P = pressure in the fixed-bed reactors, bar
P_{out} = outlet pressure of the recycle gas compressor
P_{in} = inlet pressure of the recycle gas compressor
R = universal gas constant, kJ/kmol/K
r_j = rate of reaction of the jth reaction, kmol/kg cat/s
T = temperature in the fixed-bed reactors, K
T_b = boiling point of a true boiling-point curve fraction, K
T_{inlet} = inlet temperature of the recycle gas compressor, K
t = time, h
w = weight of the catalyst, kg

Greek letters

γ = specific gravity of a true boiling-point curve function
$\gamma_{i,j}$ = stoichiometric coefficient of species i in reaction j
ΔH_{Rj} = heat of reaction of jth reaction, kcal/kmol
$\Delta H_{adiabatic}$ = adiabatic head across recycle gas compressor, kJ/kmol
ρ = density of gaseous mixture through the reactor bed, kg/m^3
ρ_c = density of the solid catalyst, kg/m^3
ϕ = bed void fraction
μ = viscosity of gas passing through the bed, Pa·s

Literature Cited

Beltramini, J. B., T. J. Wessel, and R. Datta, "Kinetics of Deactivation of Bifunctional Pt/Al_2O_3-Chlorided Catalysts by Coking," *AIChE J.*, **37**, 845 (1991).

Biegler, L. T., "Strategies for Simultaneous Solution and Optimization of Differential-Algebraic Systems," *Foundations of Computer Aided Process Design*, Elsevier, New York (1990).

Biegler, L. T., and J. E. Cuthrell, "Improved Infeasible Path Optimization for Sequential Modular Simulators—II. The Optimization Algorithm," *Comput. Chem. Eng.*, **9**, 257 (1985).

Bommannan, D., R. D. Srivastava, and D. N. Saraf, "Modeling of Catalytic Naphtha Reformers," *Can. J. Chem. Eng.*, **67**, 405 (1989).

De Pauw, R. P., and G. F. Froment, "Deactivation of a Platinum Reforming Catalyst in a Tubular Reactor," *Chem. Eng. Sci.*, **30**, 789 (1974).

Edgar, T. F., and D. M. Himmelblau, *Optimization of Chemical Processes*, McGraw-Hill, New York (1988).

Farhat, S. M., M. L. Czernicki, L. Pibouleau, and S. Domenech, "Optimization of a Multiple-fraction Batch Distillation by Non-Linear Programming," *AIChE J.*, **36**(9), 1349 (1990).

Fogler, F. S., *Elements of Chemical Reaction Engineering*, 2nd ed., Prentice Hall, NJ (1992).

Gear, C. W., *Numerical Initial Value Problems in Ordinary Differential Equations*, Prentice Hall, Englewood Clifts, NJ (1971).

Gill, P. E., W. Murray, M. A. Saunders, and M. H. Wright, *User's Guide for NPSOL (Version 4.0) A Fortran Package for Non-linear Programming*, Systems Optimization Laboratory, Stanford, CA (1986).

Hettinger, W. P., C. D. Keith, J. L. Gring, and J. W. Teter, "Hydroforming Reactions," *Ind. Eng. Chem.*, **47**(4), 719 (1955).

Holland, C., *Fundamentals of Multicomponent Distillation*, McGraw-Hill, New York, p. 18 (1981).

Kmak, W. S., "A Kinetic Simulation Model of the Powerforming Process," AIChE Meeting, Houston, TX (1972).

Krane, H. G., A. B. Groh, B. L. Schulman, and J. H. Sinfelt, "Reactions in Catalytic Reforming of Naphthas," World Petroleum Cong., (1960).

Kuo, J. W., and J. Wei, "A Lumping Analysis in Monomolecular Reaction Systems," *Ind. Eng. Fundam.*, **8**, 124 (1969).

Lion, A. K., and W. C. Edmister, "Make Equilibrium Calculations by Computer," *Hydrocarbon Proc.*, **54**(8), 119 (1975).

Little, D., *Catalytic Reforming*, Pennwell, Tulsa, OK (1985).
Macchietto, S., and I. M. Mujatba, "Design of Operation Policies for Batch Distillation," *Batch Processing Systems Engineering; Current Status and Future Direction*, G. V. Reklaitis, ed., Springer-Verlag, Berlin (1992).
Maples, R. E., *Petroleum Refining Process Economics*, Pennwell, Tulsa, OK (1983).
Marin, G. B., and G. F. Froment, "Reforming of C_6 Hydrocarbons on a Pt-Al_2O_3 Catalyst," *Chem. Eng. Sci.*, **37**(5), 759 (1982).
Marin, G. B., G. F. Froment, J. J. Lerou, and W. De Backer, "Simulation of a Catalytic Naphtha Reforming Unit," EFCE Publ. Ser., Vol. II, No. 27, C117, Paris (1983).
Mudt, T. R., T. W. Hoffmann, and S. R. Hendon, "The Closed Loop Optimization of a Semiregenerative Catalytic Reforming Process," AIChE Meeting, Houston (1995).
Nash, S., "Software Survey, NLP," *OR/MS Today*, 60 (1995).
Parera, J. M., and N. Figoli, "Reactions in Commercial Reformer," *Chem. Ind.*, **61**, 1 (1994).
Ramage, M. P., K. R. Graziani, P. H. Schipper, F. J. Krambeck, and B. C. Choi, "KINPTR (Mobil's Reforming Model), A Review of Mobil's Industrial Process Modeling Philosophy," *Adv. Chem. Eng.*, **13**, 193 (1987).
Reklaitis, G. V., *Introduction to Material and Energy Balances*, Wiley, New York (1983).
Riazi, M. R., and T. E. Daubert, "Simplify Property Predictions," *Hydrocarbon Proc.*, **59**(3), 115 (1980).
Riggs, J. B., *An Introduction to Numerical Methods for Chemical Engineers*, 2nd ed., Texas Tech University Press, Lubbock, TX (1994).
Sandler, S. A., *Chemical and Engineering Thermodynamics*, 2nd ed., Wiley, New York (1989).
Smith, R. B., "Kinetic Analysis of Naphtha Reforming with Platinum Catalyst," *Chem. Eng. Prog.*, **55**(6), 76 (1959).
Soave, G., "Equilibrium Constants from a Modified Redlich-Kwong Equation of State," *Chem. Eng. Sci.*, **27**, 1197 (1972).
Taskar, U., "Modeling and Optimization of a Naphtha Reformer," PhD Diss., Texas Tech University, Lubbock (1996).
Turpin, L. E., "Modeling of Commercial Reformers," *Chem. Ind.*, **61**, 437 (1994).
Van Trimpont, P. A., G. B. Marin, and G. F. Froment, "Reforming of C_7 Hydrocarbons on a Sulfided Commercial Pt/Al_2O_3 Catalyst," *Ind. Eng. Chem. Res.*, **27**(1), (1988).

Manuscript received June 7, 1996, and revision received Nov. 1, 1996.